ISA Transactions xxx (xxxx) xxx

Contents lists available at ScienceDirect

ISA Transactions

journal homepage: www.elsevier.com/locate/isatrans

Research article

A new modified sliding window empirical mode decomposition technique for signal carrier and harmonic separation in non-stationary signals: Application to wind turbines☆

Jack P. Salameh [a,b,*], Sebastien Cauet [a], Erik Etien [a], Anas Sakout [b], Laurent Rambault [a]

[a] LIAS-Université de Poitiers, 86000 Poitiers, France
[b] LASIE-CNRS-Université de La Rochelle, 17000 La Rochelle, France

ARTICLE INFO

Article history:
Received 1 October 2018
Received in revised form 20 November 2018
Accepted 13 December 2018
Available online xxxx

Keywords:
Signal analysis
Non-stationary
On-line analysis
EMD
SWEMD
Harmonics
Wind turbine

ABSTRACT

Modern control applications justify the need for improved techniques capable of coping with the non-stationary nature of measured signals while being able to monitor systems in real-time. Empirical Mode Decomposition (EMD) is known for its efficiency in time domain analysis of multi-component signals through Intrinsic Mode Functions (IMFs) extraction. Recent years witnessed the introduction of Sliding Window EMD (SWEMD) capable of analyzing signals in real time applications. However, complex signals require several sifting iterations while a rather increased number of IMFs might result in impracticality for on-line applications. This paper introduces a new modified faster SWEMD capable of extracting harmonics from non-stationary signals in real-time operation. The method uses the traditional EMD properties in the first pass for a small number of sifting processes. In addition, a new section is added to the algorithm based on inflection point tracking of the residue derivative from the first pass is added, in order to track low frequency waves and render the analysis faster. The method is validated for non-stationary signals with and without added colored noise and applied on measured turbine side angular velocity for harmonic extraction in wind turbines as an application. The proposed method may well be used for fault detection and disturbance rejection in mechanical systems.

1. Introduction

Environmental concerns and worldwide policies aiming to reduce greenhouse gas emission shifted the focus of generating power to renewable energy sources (hydro, solar, tidal, wind, etc.). Wind energy attracted increased attention for its abundance and the evolution of supporting technologies. Wind turbines rely on the wind speed to convert its kinetic energy into mechanical movement which finally produces electrical energy. Despite increasing global installation [1], production cost is still high compared with conventional power sources which requires greater investment leading to increased cost per unit of generated power. Moreover, high operation and maintenance costs remain a great challenge specially in off-shore wind turbines where transmission lines cost and logistical difficulties are encountered [2]. Thus the need for health/condition monitoring strategies in conjunction with advanced control methods for efficiency improvement while reducing fault occurrence rate and maintenance cost [3,4]. This extends to all kinds of systems where faults need to be detected and rejected, such as electric vehicles, robotics, etc.

Early research investigated stationary operation of wind turbines. Scenarios included constant wind speed or step changing wind speed. The aim is to study the behavior of wind turbines under different faulty conditions. Traditional signal processing techniques have been extensively used in the literature while some advanced techniques were developed to cope with the research at hand [5]. However, real time operation sees randomly changing conditions and factors. In fact, factors influencing the wind turbine operation such as weather, temperature, wind speed, load, etc. are unpredictable and non-stationary processes. In this case, conventional signal processing methods such as the Fast Fourier Transform (FFT) became inefficient in meeting system requirement for non-stationary applications. In this prospect, harmonic and oscillation detection is used by operators to assist control loops in compensating unwanted harmonics in the system. Existing oscillation detection and isolation techniques in the literature can be divided into on-line and off-line techniques for stationary and non-stationary systems. Off-line methods include Integral Absolute Error (IAE) [6], Auto covariance Function (ACF) [7], spectral envelope method [8]. Recent off-line methods for non-stationary signals include but not limited to Wavelet Transform, Discrete

☆ Research reported in this publication was supported by FEDER Program Poitou-Charentes of the European Union under award number PC158.

* Corresponding author at: LIAS-Université de Poitiers, 86000 Poitiers, France.
E-mail addresses: jacksalameh@live.com, jack.salameh@univ-poitiers.fr (J.P. Salameh).

https://doi.org/10.1016/j.isatra.2018.12.019
0019-0578/

Cosine Transform (DCT) [9], and Empirical Mode Decomposition (EMD) [10].

Despite good harmonic tracking and efficiency in signal processing and research applications, the aforementioned off-line techniques needed upgrading for on-line use. Most off-line techniques can be implemented on-line while using sliding windows. Methods with sliding windows are being used to cope with instantaneous signal characteristics change. Sliding window approaches include but are not limited to EMD [11], DCT [12]. The EMD was proposed by Huang [13] for nonlinear and non-stationary signals. The EMD breaks non-stationary signals into mono-components known as Intrinsic Mode Functions (IMFs). However, for great amount of data the EMD is time consuming, while spline interpolation requires a lot of computational effort, and over-sifting occurs. Thus, the need for modified versions to counter these drawbacks. FastEMD was introduced in [14] where matrix-free moving least squares approximation is used. Raised cosine filter proved to be faster than the EMD with lower sampling rate [15,16], while good performance was encountered for short signals and windowed version [17]. On the other hand, blockwise EMD applications [18–20] are gaining much interest for real time applications. In addition, new methods based on entropy indices were proposed in [21], along with Complete Ensemble EMD (CEEMD) [22] where faults were detected based on up to 7 IMF functions. This leaves other harmonic components out of the analysis which may represent other kinds of faults. Thus the need to put together a fast method capable of guaranteeing all harmonic extraction. Merging the analysis of two consecutive blocks is prone to discontinuities known as the "end effect". Several applications for Sliding Window EMD (SWEMD) have been developed in the literature to reduce discontinuities [11,23,24]. This paper proposes a new on-line modified SWEMD capable of separating the carrier wave of a signal from its added harmonics. It has the aim to helping control strategies in better rejecting system disturbances based on a good harmonic isolation or extraction.

On-line applications require speed and efficiency in signal analysis to cope with constantly incoming data. The traditional EMD requires several sifting processes to complete full multi-component isolation. Moreover, new sliding window techniques are using data buffering with end effect reduction through extrapolation and mirroring. This method aims to separate the carrier wave and signal frequency components while reducing the processing time. The method takes the property of the traditional EMD in separating carrier wave and harmonics of a signal, then uses it in Pass 1 with a limited number of sifting processes (up to 4–5 in the worst cases with remarkable added noise, versus 14–15 sifting processes in the traditional case). Then in Pass 2, inflection points of the derivative of the residue found in Pass 1 are tracked in order to extract the low frequency wave of Pass 1 residue. This will ensure complete separation of carrier and harmonic components of the signal. To ensure discontinuity elimination between consecutive windows in the online application, a new end effect method is employed based on the time index. The method guarantees computational cost reduction since less time is required for window analysis, while preserving all signal characteristic for analysis. The method allows control units detection of fault signatures as well as disturbance rejection in multiple applications. Section 2 presents the traditional EMD method. Section 3 introduces the new modified SWEMD along with its advantages in comparison with the traditional and other SWEMDs applied in the literature. Different signal examples are analyzed and discussed in order to highlight the purpose the proposed method. Section 4 applies the method for non-stationary signals through an application for wind turbine angular velocity harmonic detection. Section 5 discusses and concludes based on the material and results presented through this paper while introducing the future work and its aims.

2. Traditional EMD technique and algorithm

Consider a portion $x(t)$ of a signal $\chi(t)$ extracted between t^- and t^+ where two consecutive extrema (minima or maxima) are located. $x(t)$ corresponds to an oscillation starting at a minimum or maximum passing through a maximum or a minimum and ending at a minimum or maximum respectively. This represents the high frequency wave variations in $x(t)$ and denoted as $imf(t)$. In addition, let $r(t)$ represent the low frequency wave variations or local trend in $x(t)$. One can write $\chi(t) = imf(t) + r(t)$ for $t \in [t^-, t^+]$. $r(t)$ is known as the residual, which can be a first-order or slowly varying trend. The high frequency wave $imf(t)$ satisfies the properties of an Intrinsic Mode Function (IMF) proposed by Huang et al. [13]:

- The number of maxima and minima points must be equal or differ by one from the number of zero-crossings.
- The signal must have a zero mean, in other words the amplitude between each consecutive maxima and minima point must be symmetric.

The EMD aims to decompose the signal into a set of IMFs meeting the aforementioned properties. It serves the purpose of separating the high frequency wave from the signal, while making the separated oscillation modes symmetric. If $imf_1(t)$ is the first IMF of $\chi(t)$, then $imf_1(t)$ represents the high frequency wave. This accomplished through the detection of local maxima and minima points respectively. Once the extremas are found, an upper envelope connecting the maxima, and a lower envelope connecting the minima are obtained through a spline interpolation between those points. The average of both upper and lower envelopes deduces the non-constant mean. Subtracting the computed non-constant mean from the analyzed signal based gives the IMF $imf_1(t)$. Thus, the residue $r_1(t)$ is obtained based on Eq. (1).

$$\chi(t) - imf_1(t) = r_1(t) \tag{1}$$

The EMD algorithm may be summarized as follows:

1. Detect all extremas in $\chi(t)$.
2. Use spline interpolation to connect all maxima points and form the upper envelope denoted as $\chi_{max}(t)$.
3. Use spline interpolation to connect all minima points and form the lower envelope denoted as $\chi_{min}(t)$.
4. Compute the average or mean denoted by $m(t)$ such that $m(t) = \frac{\chi_{max}(t)+\chi_{min}(t)}{2}$.
5. Find the IMF $imf_1(t)$ such that $imf_1(t) = \chi(t) - m(t)$.
   The above steps are called the sifting process.
6. $imf_1(t)$ is considered the input for the next sifting process. Envelopes and $m(t)$ of $imf_1(t)$ are deduced and this value is subtracted from $imf_1(t)$ such that $imf_1(t) := imf_1(t) - m(t)$. The sifting process keeps iterating until the properties for the IMF are fulfilled.
7. Reduce the original signal $\chi(t)$ by the first mode such that $r_1(t) = \chi(t) - IMF_1(t)$.
8. Residue $r_1(t)$ is considered the input data for the second IMF. The process is repeated until all IMFs are extracted such that $r_i(t) = r_{i-1}(t) - imf_i(t)$.

The algorithm ends when no further IMFs can be extracted, i.e the residual no longer contains extrema points. One can conclude that the EMD dissects the signals into a set of components with frequency characteristics in the descending order through a set of filter banks. Finally the original signal $\chi(t)$ is decomposed such that

$$\chi(t) = r_n(t) + \sum_{i=1}^{n} imf_i(t) \tag{2}$$

where n is the number of modes. The flowchart for the EMD algorithm is found in Fig. 1.

Please cite this article as: J.P. Salameh, S. Cauet, E. Etien et al. A new modified sliding window empirical mode decomposition technique for signal carrier and harmonic separation in non-stationary signals: Application to wind turbines. ISA Transactions (2019), https://doi.org/10.1016/j.isatra.2018.12.019.

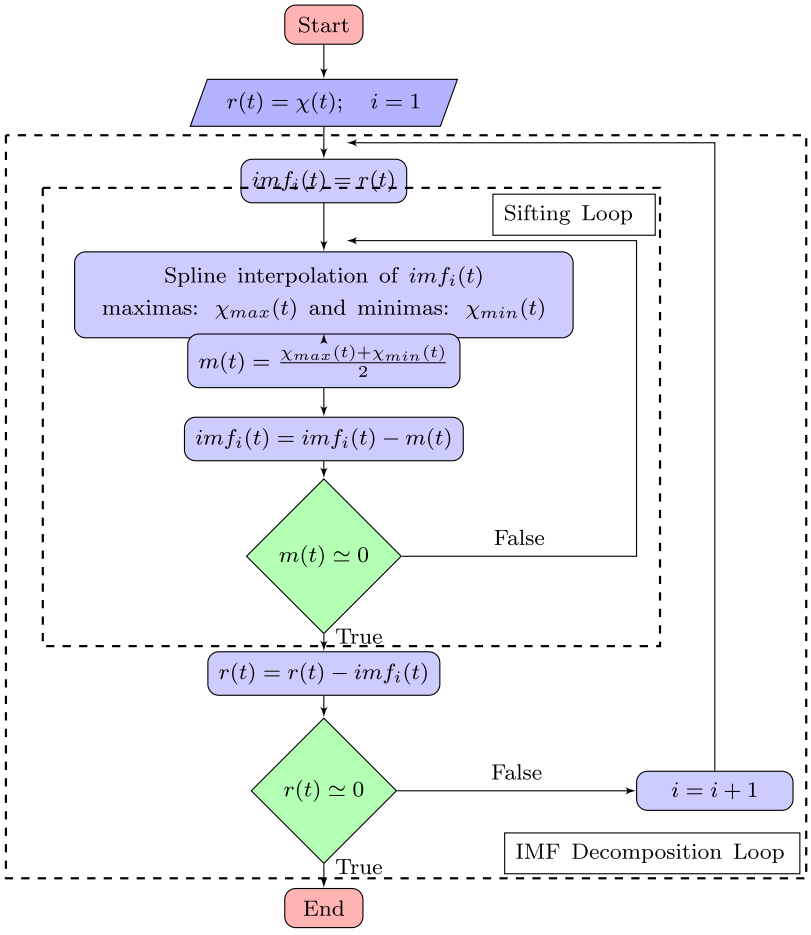

Fig. 1. Flowchart for EMD algorithm.

3. Modified on-line SWEMD

3.1. Introduction

Traditional signal processing techniques have limited time-frequency resolution. The FFT shows good time resolution in small sized-windows, while good frequency resolution is recorded in big sized windows. In addition, the Wavelet Transform (WT) has a great computational cost reduces its efficiency for real time applications. Since EMD methods rely on the time domain signal representation, the frequency resolution issue is no longer a concern. Consider the illustrative example for $\chi(t) = x_1(t) + x_2(t)$, where $x_1(t) = sin(10t) + sin(30t)$ and $x_2(t) = sin(5t)$. The signal $\chi(t)$ and its corresponding EMD decomposition is found in Fig. 2. One can note that the algorithm stopped when no extremas are detected. The decomposition shows a decreasing frequency value component the closer the algorithm reaches the end. By adding all IMF signals one can visualize the harmonic components of the original signals. However, with the traditional EMD seven sifting iterations were required for full harmonics extraction and in on-line applications for several data windows it would be time consuming. This is the first drawback tackled by the proposed method.

Fig. 3 is an illustrative example of an EMD application for carrier and high frequency components separation in a signal. Some on-line applications are fixing the number of sifting iterations in order to prevent over-sifting in some cases. However, such a constraint might well leave some low frequency components un-extracted. Thus the need for an approach capable of applying a definitive number of sifting iterations while reducing time consumption and guaranteeing full harmonic extraction.

3.2. Problems with on-line EMD applications

All SWEMD techniques use buffers to accumulate a sufficient amount of data for analysis. The same sifting process for the offline EMD is used. The same process is repeated as long as data are being fed to the buffer. The hitch resides in guaranteeing that the following data block and analysis pick up from where the first block left off through smooth merger. The challenges encountered can be summarized as follows:

- IMFs are not the same for different iterations for each data block. Thus choosing the same number of sifting iterations is vital to guaranteeing continuous IMF connections between consecutive data blocks analysis.
- Blockwise sifting process produces end effect which are unpleasant for real-time analysis. Thus the need to eliminate them.
- When a definitive number of sifting iterations is set, some blocks will still contain low frequency waves. This problem needs to be resolved if all harmonics are to be isolated from the carrier wave.

Rilling et al. [20] determined four to ten sifting iterations as sufficient for meaningful IMF extraction. Furthermore, fewer sifting iterations reduces over-sifting while preserving the physical meaning in IMFs. Considering the end effect problem, it is known that the trend function (subtracted at each iteration from the IMF candidate function) is computed through extrema interpolation. However, extremas do not extend to the end of the data block, thus the envelope is extrapolated at its ends. Most EMD methods

Please cite this article as: J.P. Salameh, S. Cauet, E. Etien et al. A new modified sliding window empirical mode decomposition technique for signal carrier and harmonic separation in non-stationary signals: Application to wind turbines. ISA Transactions (2019), https://doi.org/10.1016/j.isatra.2018.12.019.

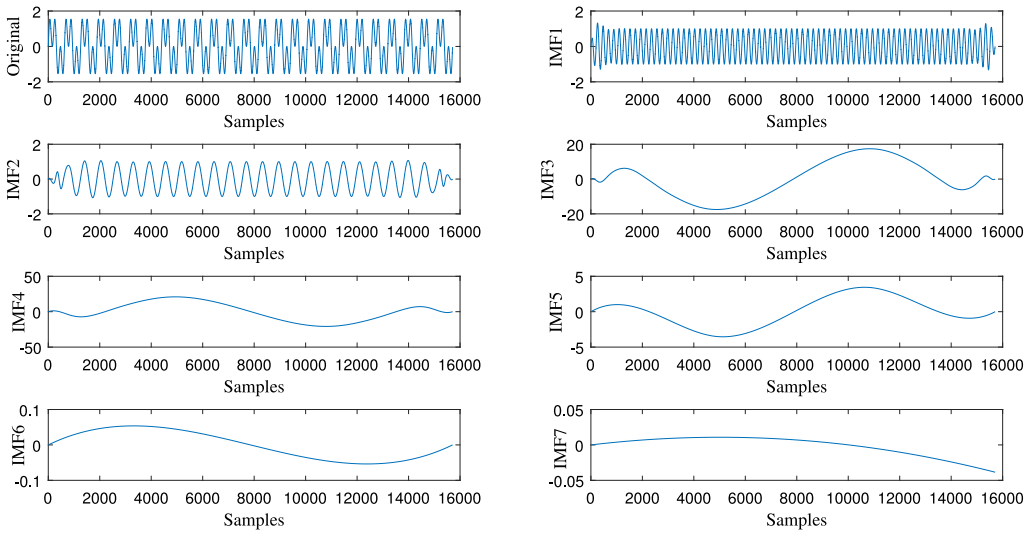

Fig. 2. EMD decomposition of $\chi(t) = x_1(t) + x_2(t)$.

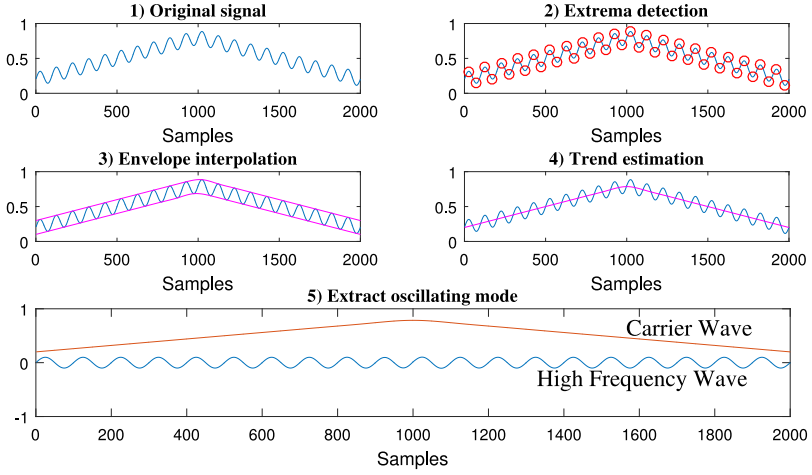

Fig. 3. EMD methodology representation.

introduce cubic splines for extrema envelopes interpolation. In cubic splines each cubic polynomial is fitted between every pair of points being interpolated. In this case the solution depends on all set of data being interpolated. Thus adding a single point, or several data points may change the entire curve, which becomes undesirable for real-time applications [25].

Hermite spline were suggested in [26], which instead forcing the continuous characteristic to the second derivative, the first derivative is fixed at each point [27]. Each spline is computed using local information only, for each point at i is estimated through averaging gradients between points $i - 1$ and $i + 1$. This indicates that only the last spline changes when points are added to the data block, while end effects can be seen only at the end of the last spline. Fig. 4 shows that end effects are limited when using Hermite interpolation even for off-line applications.

The last fix is on the level of eliminating the end effect. Rilling et al. [20] proposed extrapolation through mirroring of the last extremas. This eliminates the end effects and guarantees the smooth merging of consecutive data blocks. The modified version applied in this paper uses an overlap of data between two consecutive blocks while trimming unneeded excess. This guarantees a complete continuation of the consecutive data blocks. The trimming is based on two properties: the time index and the number of extremas sufficient and necessary to override and eliminate end effects.

3.3. Modified SWEMD for harmonic isolation and extraction

The modified SWEMD aims to separate the carrier wave from existing harmonics. The fact that some signals need several sifting loops in order to extract all containing components, while others even after specifying the number of sifting iterations still containing harmonic components requires a new method.

In this paper, the proposed SWEMD uses the old EMD process for a first pass called Pass 1. Pass 1 requires a limited number of sifting processes. For the simple example found in Fig. 3, one sifting iteration was needed in comparison with seven for the traditional EMD method. Then the second pass called Pass 2 derives the signal while applying a Hermite interpolation in order to detect inflection points. Inflection points indicate zero crossings, thus by projecting these zero crossings to the residue from Pass 1 one can compute the envelope thus extracting all remaining low frequency waves with a major cut through in time consumption for algorithm application. The advantages of the method can be summarized as follows:

- Instead of applying four to fifteen sifting processes (based on the complexity and measurement noise existing in the signal), a limited number of sifting processes is required for Pass 1.
- The extraction of low frequency harmonics is guaranteed through Pass 2. The time needed for a whole data block

Please cite this article as: J.P. Salameh, S. Cauet, E. Etien et al. A new modified sliding window empirical mode decomposition technique for signal carrier and harmonic separation in non-stationary signals: Application to wind turbines. ISA Transactions (2019), https://doi.org/10.1016/j.isatra.2018.12.019.

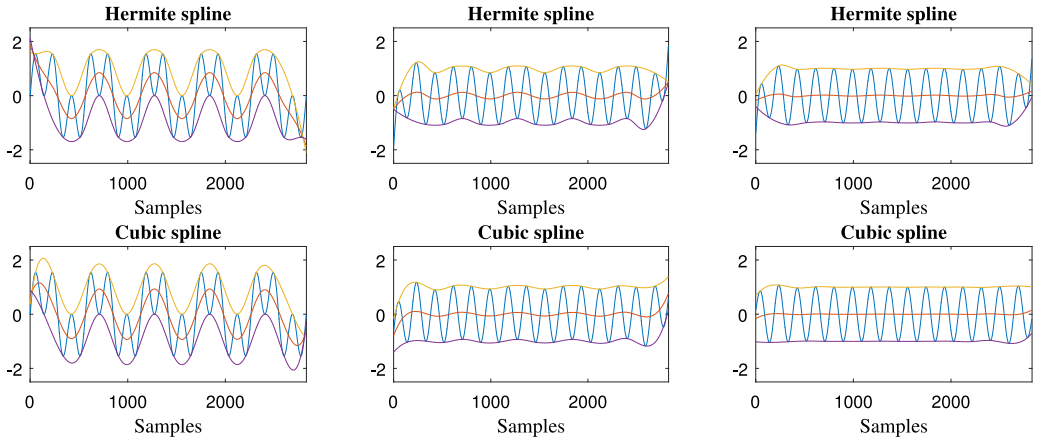

Fig. 4. Hermite (top) versus Cubic (bottom) interpolation for three IMF extraction iterations.

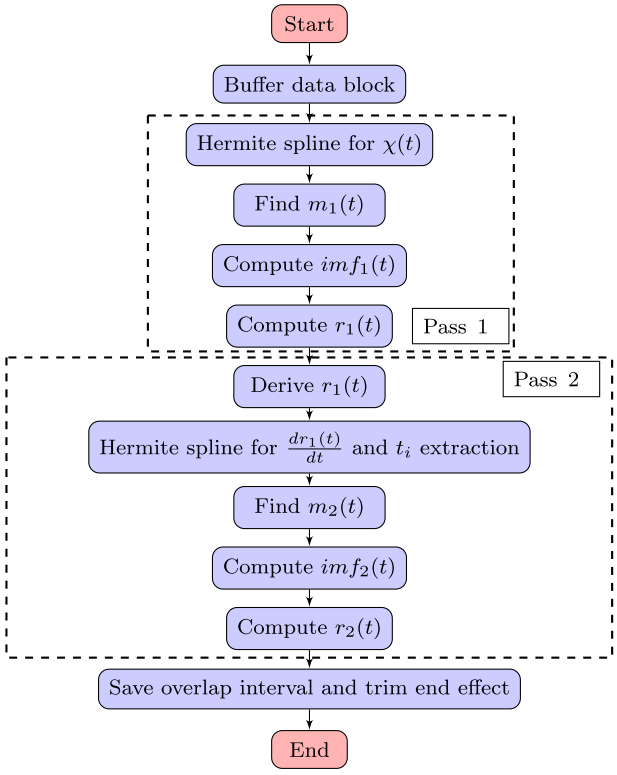

Fig. 5. Flowchart for EMD harmonic isolation.

analysis is guaranteed to be less than the time required using the traditional EMD. Thus reducing time analysis for real-time applications.

The algorithm for the proposed method is summarized as follows (see Fig. 5)

1. Buffer a set of data to form the data block.
2. Hermite spline interpolation for buffered $\chi(t)$.
3. Compute the mean

$$m_1(t) = \frac{\chi_{max}(t)+\chi_{min}(t)}{2} \tag{3}$$

4. Find the IMF for Pass 1

$$imf_1(t) = \chi(t) - m_1(t) \tag{4}$$

5. Find the residue for Pass 1

$$r_1(t) = \chi(t) - imf_1(t) \tag{5}$$

6. Derive $r_1(t)$.
7. Hermite spline interpolation for extrema detection and envelope computation for $\frac{dr_1(t)}{dt}$.
8. Extract t_i at which no end effect exists in $\frac{dr_1(t)}{dt}$ interpolation.
9. Compute the mean $m_2(t)$ for $r_1(t)$ through

$$m_2(t) = \frac{r_{1_{max}}(t)+r_{1_{min}}(t)}{2} \tag{6}$$

10. Find the IMF for Pass 2

$$imf_2(t) = r_1(t) - m_2(t) \tag{7}$$

11. Find the residue for Pass 2

$$r_2(t) = r_1(t) - imf_2(t) \tag{8}$$

12. Trim block signal at t_i.
13. Save a data interval at the end of the block, with at least seven extremas for overlap with the following data block for end effect trimming.

In order to guarantee envelope and signal continuation through consecutive blocks, seven overlap extremas are required. In this case, trimming occurs at a t_i where $\frac{dr_1(t)}{dt}$ end effects can be eliminated thus guaranteeing the elimination of those of the original signal.

3.4. The stationary case without end effect elimination

An example where each data block contains 31 400 sample is presented in Fig. 6, while only one sifting iteration and one IMF is extracted in Pass 1. One can clearly note based on (9) and (10) that all harmonics have been extracted while the carrier remains at zero.

Each block requires between 1.5 ms for analysis. However for the traditional EMD, eight sifting processes are required with a Standard Deviation (SD) of 0.3 for complete component separation while more time for analysis is required (2.3 ms). In addition, such end effects existing in the analysis cause discontinuities and unpleasant behavior even for stationary systems. In the following, the method for end effect elimination and data block merger is presented.

Please cite this article as: J.P. Salameh, S. Cauet, E. Etien et al. A new modified sliding window empirical mode decomposition technique for signal carrier and harmonic separation in non-stationary signals: Application to wind turbines. ISA Transactions (2019), https://doi.org/10.1016/j.isatra.2018.12.019.

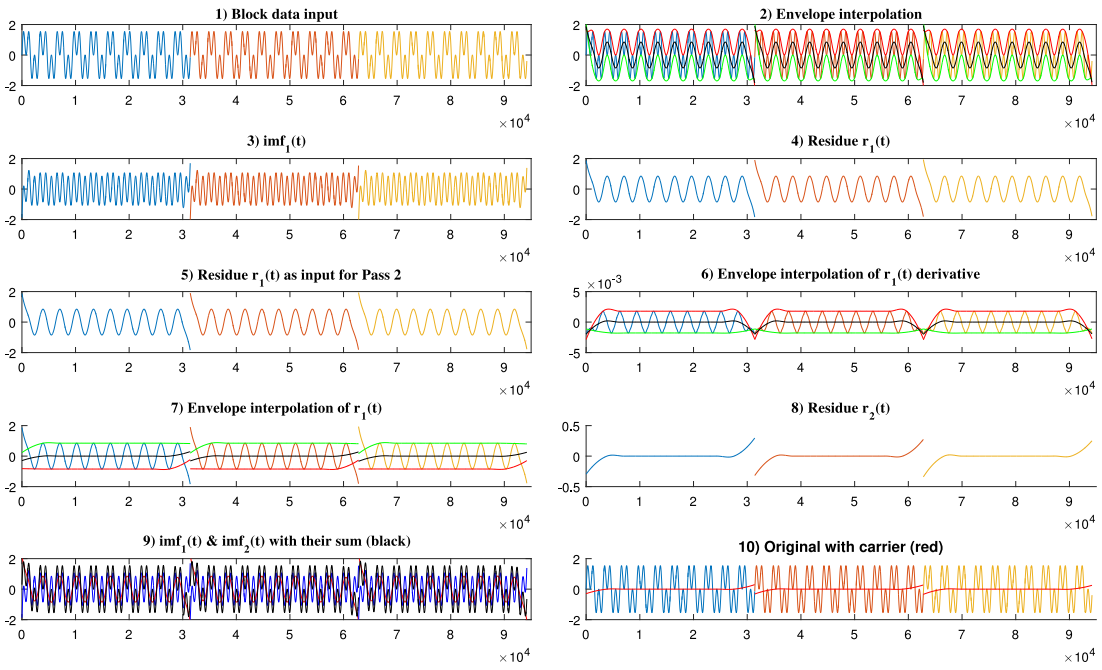

Fig. 6. On-line SWEMD without elimination of the end effect . (For interpretation of the references to color in this figure legend, the reader is referred to the web version of this article.)

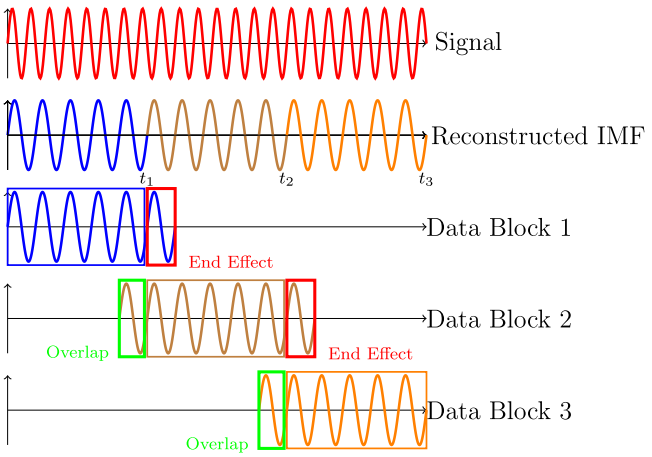

Fig. 7. End effect elimination illustrative example in blockwise (windowed) EMD . (For interpretation of the references to color in this figure legend, the reader is referred to the web version of this article.)

3.5. The stationary case with end effect elimination

Fig. 7 shows an illustrative example of the method applied with end effect elimination. For Data Block 1 only the resulting end effect at the end in the red rectangle is to be trimmed. However, for all following blocks the overlap in the green box and the end effect in the red box are to be eliminated. This is done through good extraction of time instances $t \in [t_1, \ldots, t_i]$, where $i = 1, \ldots, n$ and n is the number of data blocks. In addition, the overlap guarantees that the analysis of the following data block merges perfectly with the previous one.

Using the end effect elimination illustration in Fig. 7, one obtains the results shown in Fig. 8. It can be noted that for end effect to be eliminated one needs greater number of samples in order to guarantee both overlap and capture of t_i. It is clear that all end effects have been eliminated while perfect signal and envelope continuation are guaranteed. In addition, for 60 000 samples in this case each block needs 4.5 ms to be analyzed in the new method but 6.3 ms with the traditional EMD with the same SD. One can also note that the end effect at the beginning of the first data block has not been eliminated. This is due to the fact that no knowledge of previous extremas exists in this case.

In fact examining parts (2) and (6) in Fig. 6, it is notable that the end effect for the derivative interpolation of $r_1(t)$ is worse than that of the original block input. Thus considering a t_i at which the end effect of the derivative of the $r_1(t)$ would be eliminated will surely eliminate those in the original signal. The overlap to be chosen must take into account a sample amount greater than that of the interval in which the end effect exists.

However, this application is done for a stationary signal. To test the ability of this method for non-stationary processes, a signal with changing frequency and amplitude will be applied in the following section, while an application for wind turbine's angular velocity during non-stationary operation is presented.

4. Modified SWEMD application for non-stationary processes

4.1. Introduction

In this section, the proposed method's efficiency is tested for non-stationary signals. For that purpose, the signal in Fig. 9 is considered as a representation for speed change in wind turbines while perturbation amplitude and frequency vary. One can note 5 different intervals where the frequency components vary along with the amplitude and the offset.

The aforementioned method is applied in order to isolate the carrier wave from the harmonics. The results are shown in Fig. 10. $imf_1(t)$ shown in (3) is extracted through two sifting processes. The residue in Pass 1 $r_1(t)$ still contained the low frequency wave component, thus the need for Pass 2. After extracting the low frequency wave, the carrier is completely separated from existing harmonics found in the sum of $imf_1(t)$ and $imf_2(t)$.

Please cite this article as: J.P. Salameh, S. Cauet, E. Etien et al. A new modified sliding window empirical mode decomposition technique for signal carrier and harmonic separation in non-stationary signals: Application to wind turbines. ISA Transactions (2019), https://doi.org/10.1016/j.isatra.2018.12.019.

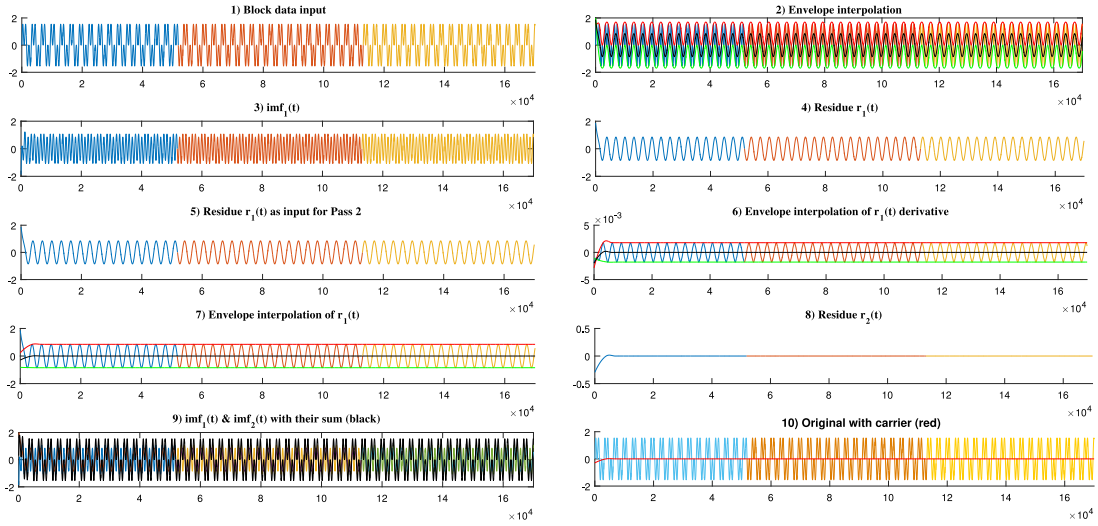

Fig. 8. On-line SWEMD with elimination of the end effect . (For interpretation of the references to color in this figure legend, the reader is referred to the web version of this article.)

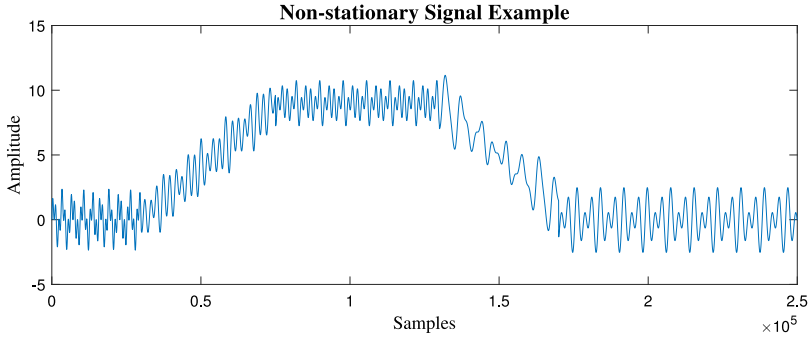

Fig. 9. Non-stationary signal example.

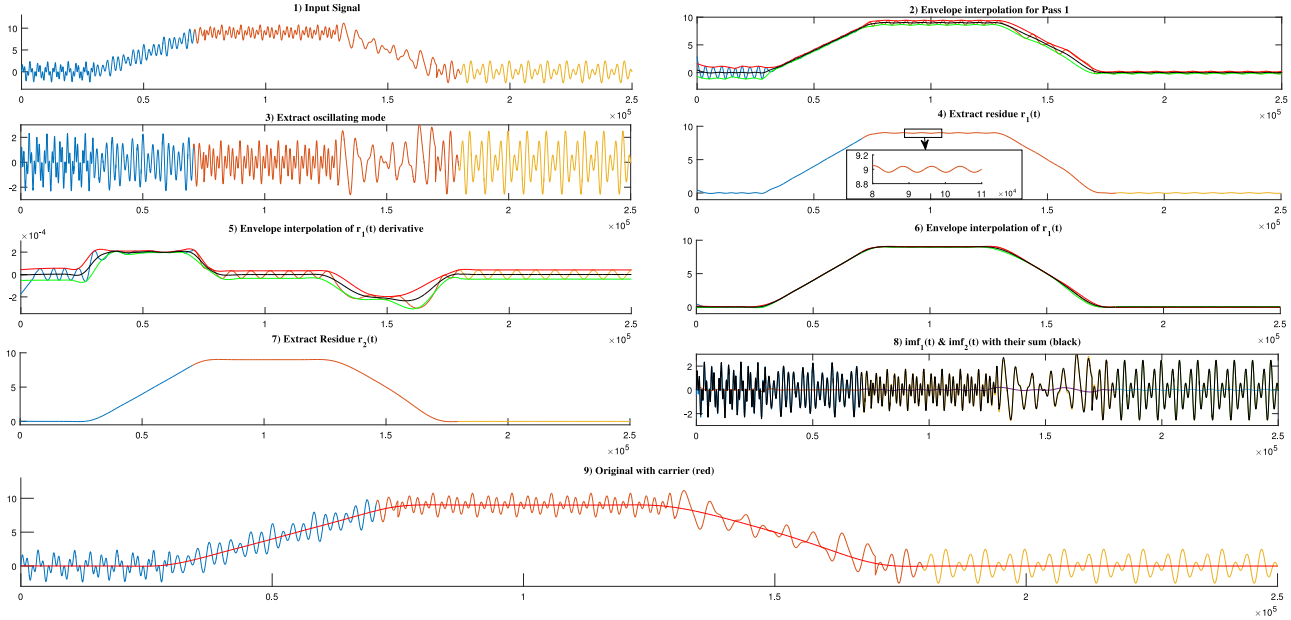

Fig. 10. Modified SWEMD applied to a non-stationary signal . (For interpretation of the references to color in this figure legend, the reader is referred to the web version of this article.)

Please cite this article as: J.P. Salameh, S. Cauet, E. Etien et al. A new modified sliding window empirical mode decomposition technique for signal carrier and harmonic separation in non-stationary signals: Application to wind turbines. ISA Transactions (2019), https://doi.org/10.1016/j.isatra.2018.12.019.

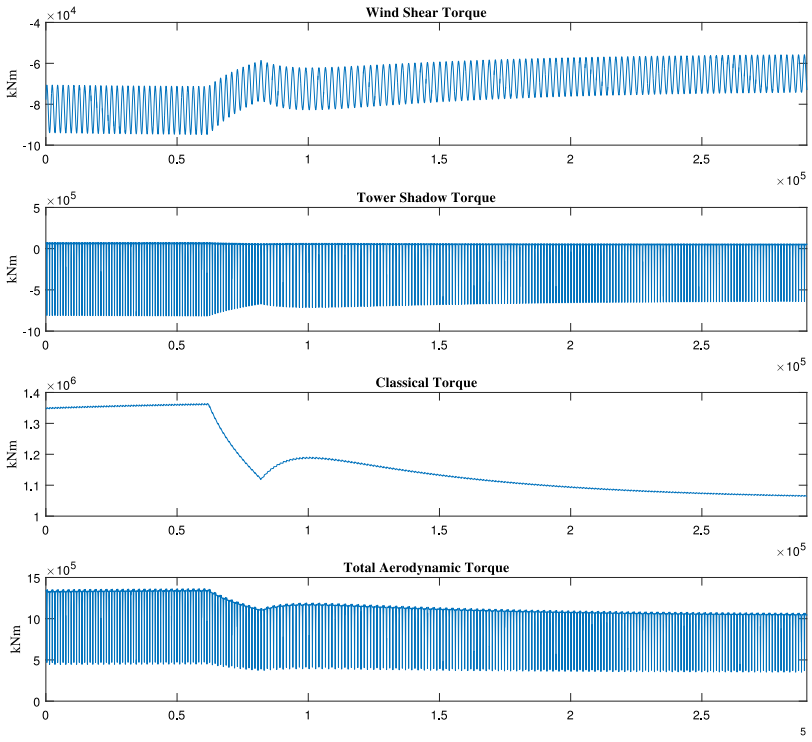

Fig. 11. Aerodynamic torque produced by the wind profile.

4.2. Harmonic extraction of turbine side angular velocity in wind turbines

Wind profiles driving wind turbines are random non-stationary processes. They introduce disturbances and harmonics which propagate along the drive train, through the gearbox, until reaching the generator and eventually the turbine current and voltage output. The total wind speed is the combination of the measured speed at the hub level along with the wind shear and tower shadow. The following wind speed and aerodynamic torque formulation is considered (see Fig. 11) [28,29]

$$v_{eq}(t,\theta) = v_{eq_0} + v_{eq_{ws}} + v_{eq_{ts}} \tag{9}$$

where the wind speed measured at the hub level v_{eq_0} is expressed as

$$v_{eq_0} = V_h \tag{10}$$

The wind shear speed component $v_{eq_{ws}}$ expression is

$$v_{eq_{ws}} = V_h\left[\frac{\alpha(\alpha-1)}{8}\left(\frac{R}{H}\right)^2 + \frac{\alpha(\alpha-1)(\alpha-2)}{60}\left(\frac{R}{H}\right)^3 cos^3 3\theta_b\right] \tag{11}$$

while the speed due to tower shadow $v_{eq_{ts}}$ is found to be

$$v_{eq_{ts}} = \frac{V_h}{3R^2}\sum_{b=1}^{3}\left[\frac{a^2}{sin^2\theta_b} ln\left(\frac{R^2 sin^2\theta_b}{x^2}+1\right) - \frac{2a^2R^2}{R^2 sin^2\theta_b + x^2}\right] \tag{12}$$

Thus the total aerodynamic T_{aero} is found to be

$$\begin{aligned} T_{aero}(t,\theta) &= \rho A V_h C_p(\lambda_0)\left[\frac{1}{2}\frac{V_h^2}{\omega_r} + \frac{R}{\lambda_0}(v_{eq_{ws}} + v_{eq_{ts}})\right] \\ &= T_{aero}^{classical} + T_{aero}^{ws} + T_{aero}^{ts} \end{aligned} \tag{13}$$

while V_h being the measured wind speed at hub level, α as the empirical wind shear exponent, R being the turbine rotor radius, H is the hub height, a as the tower radius, x being the distance of blade origin from the tower mid-line, ρ the air density, A as the area swept by the blades, C_p is the power coefficient, λ_0 being the tip speed ratio, ω_r as the rotor speed, θ_b is the blade angle position, $T_{aero}^{classical}$ being the classical torque produced by the turbines, T_{aero}^{ws} being the wind shear torque component, and T_{aero}^{ts} the tower shadow torque component. Parameters are shown in Table 1. Fig. 11 shows the different aerodynamic torque components for changing wind speed profile. One can note three types of harmonics introduced to the measured turbine side angular velocity. Disturbances are linked to the wind shear, tower shadow and speed variations respectively. The measured angular velocity is found in Fig. 12.

Table 1
Parameters values.

Parameter	Value
α	0.3
R	56 m
H	90 m
a	8 m
x	3 m
ρ	1.25 kg/m^3
Power	2.5 MW

Control strategies will always tend to eliminate the harmonics introduced to the system. The modified SWEMD will do the job in separating these harmonics from the carrier wave, thus supporting control strategies in better analyzing containing frequency components. The process bloc diagram is shown in Fig. 13.

The modified SWEMD method is applied for the measured angular velocity signal. The results are shown in Fig. 14. One sifting process was sufficient for $imf_1(t)$ extraction. Residue $r_1(t)$ still contained low frequency wave. Pass 2 extracted the remaining harmonics, while residue $r_2(t)$ is harmonics-free. It is important to note that a small deviation from the signal is encountered during sudden speed change specially at the derivative level of $r_1(t)$.

Please cite this article as: J.P. Salameh, S. Cauet, E. Etien et al. A new modified sliding window empirical mode decomposition technique for signal carrier and harmonic separation in non-stationary signals: Application to wind turbines. ISA Transactions (2019), https://doi.org/10.1016/j.isatra.2018.12.019.

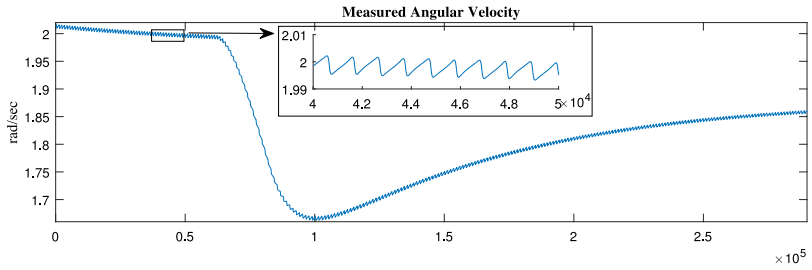

Fig. 12. Turbine side angular velocity.

However, this deviation does not influence the end result which shows complete harmonic extraction and separation from carrier. The proposed method is successful in non-stationary applications.

The last verification is applied through spectral analysis. The FFT is applied for both high speed and low speed harmonics sections found in (9) of Fig. 14. The results are shown in Fig. 15.

One can clearly note that all harmonics are preserved. In fact, apart from the carrier physical quantity, all frequency and amplitude information are well extracted. The harmonics seen in the figure are related the normal wind speed variations, in addition to the wind shear and tower shadow components. Thus a full separation of all disturbances is observed.

This proves the effectiveness of the method in separating the carrier wave from the harmonic components even for low frequency waves. In this case, the control strategy is capable of dealing with disturbance rejection either for all harmonics or the added harmonic by a fault or other exogenous factors. In addition, since all angular velocity variation have been omitted, the control unit will now be faster in dealing with harmonic rejection.

4.3. Harmonic extraction for turbine side angular velocity with added measurement colored noise

In this section added measurement noise is considered. This test proves the effectiveness of the proposed method when noise exists in the measurement. Several tests have been carried out with different colored noise. Fig. 16 shows the results in the presence of 40 dB Signal to Noise Ratio (SNR) pink noise added to the measurement.

Part (1) in Fig. 16 shows the first envelope interpolation in the first sifting process. In fact, six sifting processes were required in this case to extract all high frequency waves with an added Pass 2 were sufficient for complete carrier separation from harmonics as seen in parts (2) and (3). Compared to the traditional EMD, seventeen sifting processes were required to extract all IMFs. The computation time is cut down by 2/3 in this case. Even with colored added noise, the method guarantees complete separation between carrier and harmonic waves, while all discontinuities are eliminated through the end effect method utilized. 5.8 s were required for the 100 000 sample window in the proposed method, while the traditional EMD needed 14.3 s to complete IMF extraction.

A summary of computational time for different examples is shown in Table 2, computation time is realized on PC: Intel(R) Core(TM) i5-6600 CPU @ 3.30 GHz, 64 bits; Ram: 8 GB . The results show that the new modified EMD approach cuts down time consumption in computation process. Fewer sifting processes are required while all harmonics have been extracted. This is an advantage over the methods applied in [21,22] where detecting faults is based on up to seven IMFs only. The frequency signature extracted in this case is a reflection of any system performance. Thus enabling the control strategy to reject disturbances, and detect fault signatures no matter how small their physical value was.

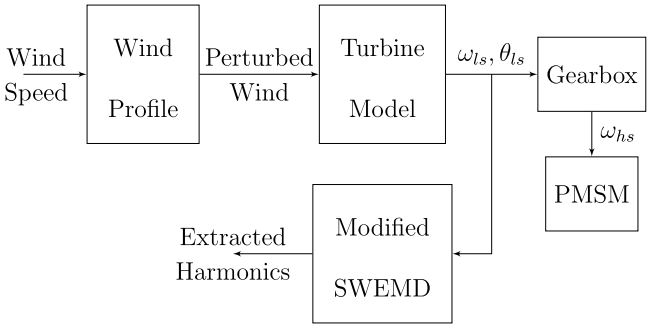

Fig. 13. Bloc Diagram of the modified SWEMD harmonics extraction for angular velocity signal.

Table 2
Process comparison for different applications for both modified and traditional EMD.

	Modified EMD		Traditional EMD	
	Sifting processes	Time	Sifting processes	Time
Stationary case	1 & 1 Pass 2	4.5 ms	7	6.3 ms
Non-stationary case	2 & 1 Pass 2	0.28 s	12	0.63 s
Measured angular velocity	3 & 1 Pass 2	2.2 s	14	4.3 s
Angular velocity with pink noise	6 & 1 Pass 2	5.8 s	17	14.3 s

5. Conclusion

Traditional signal processing methods are falling behind modern system requirements regarding non-linearity, non-stationarity, robustness, efficiency, reliability, etc. Thus, the need for new improved methods capable of extracting signal characteristics for better understanding of system operation. This paper introduces a new modified SWEMD method aiming to reduce processing time while being applied on-line. The method uses the characteristics of the traditional EMD in extracting IMFs, then applies an interpolation to the derivative of the residue obtained in the first section of the algorithm. In addition, a new approach for end effect elimination is presented based on time indices and the number of extrema chosen for data overlap. Results show efficiency and speed in real time analysis while removing end effects successfully and merging different data blocks. In fact, the method uses in worst case scenario three sifting iterations and one derivative interpolation to complete harmonic extraction. FFT analysis proves complete frequency and amplitude information extraction from the original signal.

The application for wind turbines shows the ability for applying this new modified SWEMD on real systems. Furthermore, it can be used as control strategy assistance for disturbance rejection of harmonic compensation. Future work includes the application of this method along with an Active Disturbance Rejection Control (ADRC) strategy for harmonic rejection in wind turbines. In addition, a factor needs to be added similar to the standard deviation in

Please cite this article as: J.P. Salameh, S. Cauet, E. Etien et al. A new modified sliding window empirical mode decomposition technique for signal carrier and harmonic separation in non-stationary signals: Application to wind turbines. ISA Transactions (2019), https://doi.org/10.1016/j.isatra.2018.12.019.

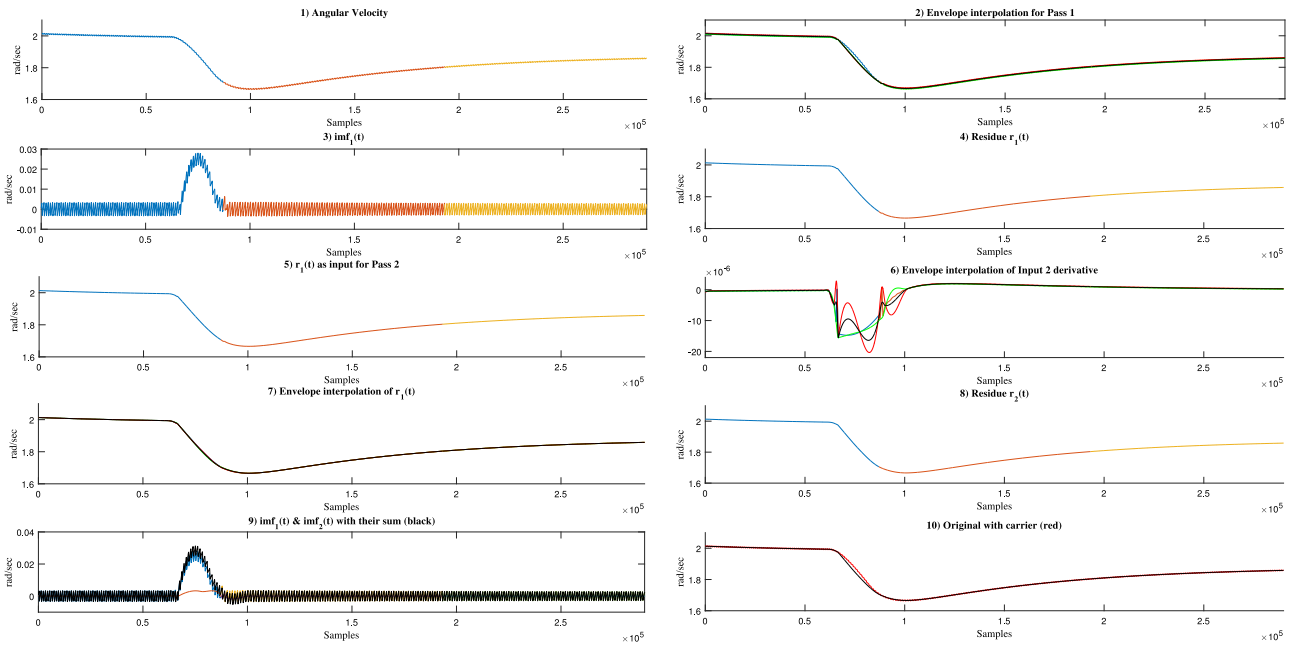

Fig. 14. Modified SWEMD applied for angular velocity harmonics extraction . (For interpretation of the references to color in this figure legend, the reader is referred to the web version of this article.)

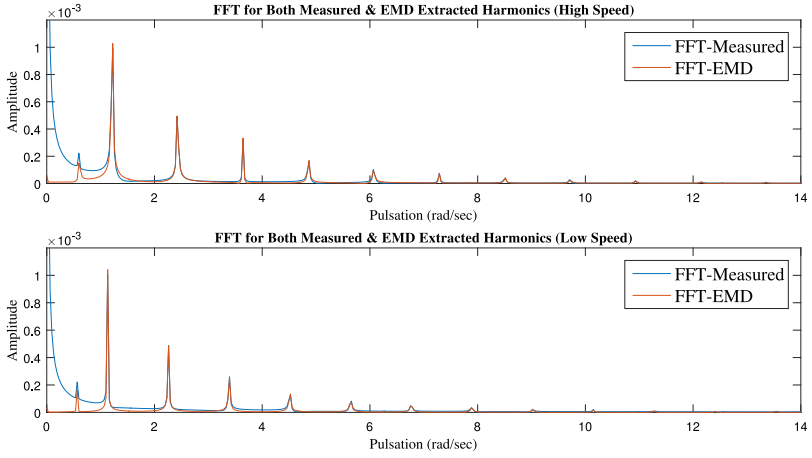

Fig. 15. FFT comparison between the original signal and its extracted harmonics through EMD (High speed section on top, Low speed section at the bottom).

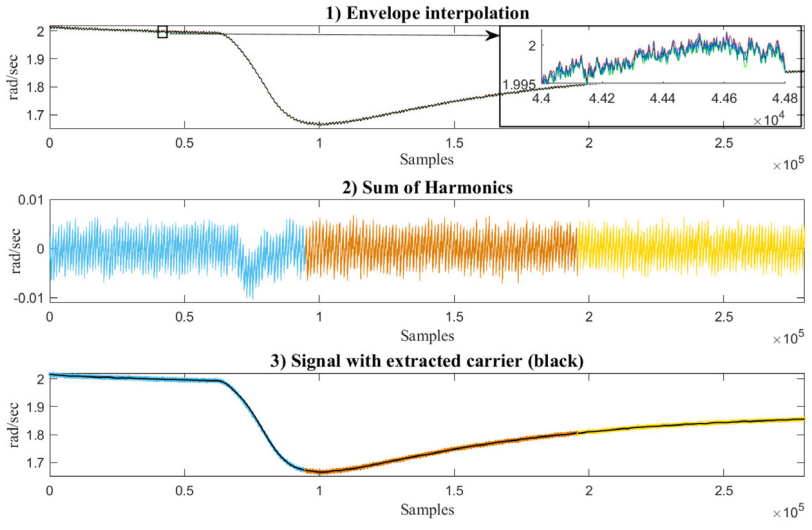

Fig. 16. Modified EMD for the turbine side angular velocity measurement with added pink noise.

order to find the sufficient necessary number of sifting processes applied in Pass 1, before applying Pass2. Without the factor, one needs to fix the number of sifting processes before applying the algorithm and this number changes in different applications.

Acknowledgment

Research reported in this publication was supported by FEDER Program Poitou-Charentes of the European Union under award number PC158.

References

[1] GWEC, GWEC Global wind report: Annual market update 2015, URL http://gwec.net/global-figures/graphs/ [Accessed 18.05.17].
[2] Salameh JP, Cauet S, Etien E, Sakout A, Rambault L. Gearbox condition monitoring in wind turbines: A review. Mech Syst Signal Process 2018;111:251–64. http://dx.doi.org/10.1016/j.ymssp.2018.03.052.
[3] Njiri JG, Sffker D. State-of-the-art in wind turbine control: Trends and challenges. Renew Sustain Energy Rev 2016;60:377–93. http://dx.doi.org/10.1016/j.rser.2016.01.110.
[4] Mohanty AR. Machinery condition monitoring principles and practices. CRS Press, Taylor & Francis Group; 2015.
[5] Randall RB. Vibration-based condition monitoring: industrial, aerospace and automotive applications. John Wiley & Sons; 2011.
[6] Hgglund T. A control-loop performance monitor. Control Eng Pract 1995;3(11):1543–51. http://dx.doi.org/10.1016/0967-0661(95)00164-P.
[7] Thornhill N, Huang B, Zhang H. Detection of multiple oscillations in control loops. J Process Control 2003;13(1):91–100. http://dx.doi.org/10.1016/S0959-1524(02)00007-0.
[8] Jiang H, Choudhury MS, Shah SL, Cox JW, Paulonis MA. Detection and diagnosis of plant-wide oscillations using the spectral envelope method. IFAC Proc Vol 2006;39(2):1139–44. http://dx.doi.org/10.3182/20060402-4-BR-2902.01139, 6th IFAC Symposium on Advanced Control of Chemical Processes.
[9] Li X, Wang J, Huang B, Lu S. The dct-based oscillation detection method for a single time series. J Process Control 2010;20(5):609–17.
[10] Braun S, Feldman M. Decomposition of non-stationary signals into varying time scales: some aspects of the emd and hvd methods. Mech Syst Signal Process 2011;25(7):2608–30.
[11] Fontugne R, Borgnat P, Flandrin P. Online empirical mode decomposition. In: Acoustics, speech and signal processing (ICASSP), 2017 IEEE international conference on. IEEE; 2017, p. 4306–10.
[12] Wang J, Huang B, Lu S. Improved dct-based method for online detection of oscillations in univariate time series. Control Eng Pract 2013;21(5):622–30.
[13] Huang NE, Shen Z, Long SR, Wu MC, Shih HH, Zheng Q, Yen NC, Tung CC, Liu HH. The empirical mode decomposition and the Hilbert spectrum for nonlinear and non-stationary time series analysis. Proc. R. Soc. Lond. A: Math. Phys. Eng. Sci. 1998;454(1971):903–95. http://dx.doi.org/10.1098/rspa.1998.0193.
[14] Blakely CD. A fast empirical mode decomposition technique for nonstationary nonlinear time series, Vol. 3. Elsevier Science; 2005, Preprint submitted for publication.
[15] Roy A, Doherty JF. Raised cosine interpolation for empirical mode decomposition. In: Information sciences and systems, 2009. CISS 2009. 43rd annual conference on. IEEE; 2009, p. 888–92.
[16] Roy A, Doherty JF. Improved signal analysis performance at low sampling rates using raised cosine empirical mode decomposition. Electron Lett 2010;46(2):176–7.
[17] Roy A, Doherty JF. Raised cosine filter-based empirical mode decomposition. IET Signal Process 2011;5(2):121–9.
[18] Trnka P, Hofreiter M. The empirical mode decomposition in real-time. In: Proceedings of the 18th international conference on process control, Tatranská Lomnica, Slovakia. 2011, p. 14–7.
[19] Zarraga FL. On-line extraction of modal characteristics from power system measurements based on Hilbert-Huang analysis. In: Electrical engineering, computing science and automatic control, CCE, 2009 6th international conference on. IEEE; 2009, p. 1–6.
[20] Rilling G, Flandrin P, Goncalves P, et al. On empirical mode decomposition and its algorithms. In: IEEE-EURASIP workshop on nonlinear signal and image processing, Vol. 3. NSIP-03, Grado (I); 2003, p. 8–11.
[21] Alvarez-Monroy G, Mejia-Barron A, Rodriguez MV, Granados-Lieberman D, Olivares-Galvan JC, Escarela-Perez R. A new EMD-Shannon entropy-based methodology for detection of inter-turn faults in transformers. In: Power, electronics and computing (ROPEC), 2017 IEEE international autumn meeting on. IEEE; 2017, p. 1–6.
[22] Mejia-Barron A, Valtierra-Rodriguez M, Granados-Lieberman D, Olivares-Galvan JC, Escarela-Perez R. The application of EMD-based methods for diagnosis of winding faults in a transformer using transient and steady state currents. Measurement 2018;117:371–9.
[23] Faltermeier R, Zeiler A, Tomé AM, Brawanski A, Lang EW. Weighted sliding empirical mode decomposition. Adv Adapt Data Anal 2011;3(04):509–26.
[24] Zeiler A, Faltermeier R, Tomé AM, Puntonet C, Brawanski A, Lang EW. Weighted sliding empirical mode decomposition for online analysis of biomedical time series. Neural Process Lett 2013;37(1):21–32.
[25] Knott GD. Interpolating cubic splines, Vol. 18. Springer Science & Business Media; 2012.
[26] Meeson RN. Hht sifting and adaptive filtering, Tech.rep., Institute for Defense Analyses Alexandria Va (2003).
[27] Cheney E, Kincaid D. Numerical mathematics and computing. Nelson Education; 2012.
[28] Sørensen P, Hansen AD, Rosas PAC. Wind models for simulation of power fluctuations from wind farms. J. Wind Eng Ind Aerodyn 2002;90(12–15):1381–402.
[29] Santoso S, Le HT. Fundamental time–domain wind turbine models for wind power studies. Renew Energy 2007;32(14):2436–52.